Journal of Polymer Research (2024) 31:192
https://doi.org/10.1007/s10965-024-04024-1

ORIGINAL PAPER

# Effect of UV-induced crosslink network structure on the properties of polylactic acid/polybutylene adipate terephthalate blend

Xueyan Bian[1] · Suju Fan[1] · Gang Xia[1] · John H. Xin[1] · Shouxiang Jiang[1]

Received: 28 February 2024 / Accepted: 24 May 2024
© The Author(s) 2024

## Abstract

Over the past few decades, biobased polylactic acid (PLA) has emerged as the most promising option to replace some of the fossil-based and nonbiodegradable polymers due to environmental concerns. In this study, a flexible polymer, polybutylene adipate terephthalate (PBAT) was blended with PLA to improve the toughness and flexibility of PLA, and the PLA/PBAT blend was further UV-induced to form crosslink structure. The results show that the flexibility and toughness of PLA could be significantly enhanced when PBAT was introduced, and the compatibility of PLA and PBAT could be enhanced by the development of a crosslink structure. Especially, the elongation at break and unnotched impact strength of ABT-UV30 (PLA/PBAT/triallyisocyanurate (TAIC) exposed to ultraviolet (UV) light for 30 min) was increased to 3.9 and 8.4 times of neat PLA. The glass transition temperature (Tg) of PLA was increased from 63.4 to 72.9 °C as the radiation duration was prolonged to 60 min. The melting point temperature of PBAT was also increased gradually until it eventually coincided with that of PLA. The thermalgravimetric analyzer thermograms show that a moderate amount of UV radiation can improve the thermal stability of the sample while an excessive amount of UV radiation can reduce the degradation temperature.

**Keywords** Biodegradable · Polylactic acid · Polybutylene adipate terephthalate · Crosslinked structure

## Introduction

Plastic production expanded quickly after World War II, dramatically improving people's lives, and transforming contemporary society. However, most plastic products are derived from fossil fuels and cannot be biodegraded. It is estimated that about 6.3 billion Mt of plastic waste had been produced by 2015, but only 9% of this plastic waste were recycled, leaving 91% to be burned, landfilled or left in the natural environment [1]. Over the past few decades, there has been an increasing interest in using biobased polymers with potential degradability to replace certain fossil-derived polymers, which would significantly reduce the consumption of natural resources and decrease environmental pollutants. Energy crops, food-based biomass waste, agricultural biomass residue, and forest biomass are the main sources of biobased polymers [2].

Polylactic acid (PLA) is an aliphatic polyester, primarily produced by the ring-opening polymerization of lactide and industrial polycondensation of lactic acid. The basic unit of PLA, lactic acid, is produced from renewable resources such as wheat, straw, corn, and sorghum, which is bio-based and can be decomposed into water and carbon dioxide by microbes. Compared to other biobased or biodegradable polymers such as poly (hydroxy valerate) (PHV), poly (hydroxy butyrate) (PHB), polycaprolactone (PCL), polybutylene succinate (PBS) and polybutylene adipate terephthalate (PBAT), PLA has a better overall performance in terms of tensile strength, modulus, thermoplastic performance, and ability to be molded by using different processes [3]. However, PLA has some intrinsic shortcomings, such as rigidity, brittleness, low thermal stability and poor processability, which greatly limit its applications [4–6].

To date, several approaches have been proposed to address these shortcomings, such as forming a stereocomplex (SC) structure, adding nucleating agents, promoting a crosslink reaction, plasticization, and blending with various tough polymers [6–9]. Ikada et al. first reported that

✉ John H. Xin
john.xin@polyu.edu.hk

✉ Shouxiang Jiang
kinor.j@polyu.edu.hk

[1] School of Fashion and Textiles, The Hong Kong Polytechnic University, Hung Hom, Kowloon 999077, Hong Kong, China

Published online: 20 June 2024

poly (l-lactic acid) (PLLA) and poly (d-lactic acid) (PDLA) blended with a ratio of 1:1 can produce a SC crystallite structure. The SC crystallite has a melting point temperature (Tm) of about 230 °C, which is 50 °C higher than that of the PLLA or PDLA homocrystals [10]. However, the high cost of high-purity PDLA prevents its wide use in industrial production. According to the study from Tang' group, the addition of a nucleating agent, ethylenebishydroxystearamide (EBH), can considerably increase the crystallinity and crystallization rate of PLA. After the annealing procedure, the heat deflection temperature (HDT) of nucleated PLA can be increased by 30 °C [11]. Shaffer et al. has used two crosslinking agents, trimethylolpropane triacrylate (TMPTA) and triallyisocyanurate (TAIC) to modify PLA. It was reported that a crosslinking reaction that occurred close to the glass transition temperature (Tg) can significantly enhance the thermomechanical properties of the PLA polymer [12]. Tsou et al. prepared PLA with adipate ester as a plasticizer and concluded that the addition of adipate ester could improve the toughness of PLA, but reduced the cold crystallization and Tg [13].

Polymer blends are considered as materials with tunable qualities that can deliver a synergistic performance. Kobayashi et al. blended PLA with different polymers including polyethylene terephthalate (PET), polybutylene terephthalate (PBT), nylon (N6), nylon (N12), and polycarbonate (PC). The results indicated that both the tensile strength, elongation at break and HDT of these blends (with a PLA/polymer ratio of 80/20) were increased significantly [14]. However, these blends cannot be fully biodegraded due to the addition of fossil-based and nonbiodegradable polymers. Therefore, increasing attention has been attracted to modify PLA with biodegradable materials. PBAT is fossil-based but a fully biodegradable polymer. Compared to other biopolymers such as poly (hydroxy valerate) (PHV), poly (hydroxy butyrate) (PHB), polycaprolactone (PCL), and polybutylene succinate (PBS), PBAT is fossil-based but a fully biodegradable polymer that has high elongation at break and impact strength compared to other biopolymers. PBAT is therefore considered as a promising polymer to enhance the flexibility and toughness of PLA [15]. However, the incompatibility between PLA and PBAT can cause interfacial separation, leading to an unsatisfactory enhancement in mechanical properties [16].

In this study, PBAT was added to improve the flexibility and toughness of PLA. The compatibility of PLA and PBAT was enhanced through the formation of the crosslink spatial network. Triallyisocyanurate (TAIC) was used as the crosslinking agent, and ultraviolet (UV) radiation was employed to induce the occurrence of crosslink reaction. The morphology, mechanical performance, phase transition temperature, and thermogravimetric analysis of samples were then evaluated, and the mechanisms were also investigated.

## Experimental

### Materials

PLA was supplied by Anhui Fengyuan Bio-Fiber Co., Ltd. The PLA polymer has an average molecular weight of approximately 120,000 g/mol, a density of 1.24 g/cm$^3$, and a melt mass-flow rate (MFR) of 4 g/10 min (190 °C/2.16 kg).

PBAT was purchased from Shanghai Macklin Biochemical Co., Ltd. The PBAT polymer has an average molecular weight of approximately 680,000 g/mol, a density of 1.21 g/cm$^3$, and a MFR of 4.5 g/10 min (190 °C/2.16 kg).

TAIC ($C_{12}H_{15}N_3O_3$), with a molecular weight of 249.27, was supplied by Thermo Fisher Scientific (USA). The TAIC's density is 0.45 g/cm$^3$.

Dichloromethane (DCM), HPLC grade was purchase from Anaqua Global International Inc. Limited. The DCM's density is about 1.33 g/cm$^3$(20 ± 4 °C).

### Sample preparation

PLA and PBAT polymer masterbatches were immersed into an ultrasonic ethanol bath for 30 min to remove impurities, then rinsed five times with distilled water. Prior to usage, the cleaned masterbatches were dried in a vacuum oven at 60 °C for 24 h to eliminate surface moisture. An organic solvent, DCM, was used to dissolve a certain mass of PLA, PBAT, and PLA/PBAT blend polymers (weight ratio: 80/20) at a mass fraction of 10%. The PLA, PBAT, and PLA/PBAT solutions were stirred by using a magnetic stirrer at a temperature of 40 °C, and all the PLA and PBAT polymer masterbatches were completely dissolved after a 60-minute of stirring at a rotational speed of 500 rpm.

The fully dissolved PLA/PBAT solution was poured into six transparent bottles. Five of them were added to TAIC at a mass percentage of 3% (to polymers) and stirred for 10 more minutes so that the TAIC could disperse uniformly in the solution. Then four bottles filled with the PLA/PBAT/TAIC solutions were placed in a UV light box (mode: fluorescent lamp, supported by Shanghai Xinxin Light Co., Ltd.) and exposed to UV light for various lengths of time—15, 30, 45, and 60 min. The UV-induced cross-linking reaction is completed under the operation of 5 UV lamps, with each lamp wavelength of between 100 ~ 400 nm, power of 15 w, and intensity of 45 uw/cm$^2$. The radiation distance is around 23 ~ 25 cm. Following UV exposure, all the solutions were used to cast films, and kept in a fume hood for 2 hours to allow the DCM solvent to evaporate. Then, all the films were dried in a vacuum oven to further remove any residual DCM. The preparation recipe is shown in Table 1.

All the samples were hot-pressed into sheets by using a compression molding machine (model: ZS-406B,

**Table 1** Preparation recipe of samples

| Sample Name | Weight $_{PLA}$ (g) | Weight $_{PBAT}$ (g) | Weight $_{TAIC}$ (g) | Weight $_{DCM}$ (g) | UV radiation (min) |
|---|---|---|---|---|---|
| PLA | 10 | 0 | 0 | 90 | 0 |
| PBAT | 0 | 10 | 0 | 90 | 0 |
| AB | 8 | 2 | 0 | 90 | 0 |
| ABT-UV0 | 8 | 2 | 0.3 | 90 | 0 |
| ABT-UV15 | 8 | 2 | 0.3 | 90 | 15 |
| ABT-UV30 | 8 | 2 | 0.3 | 90 | 30 |
| ABT-UV45 | 8 | 2 | 0.3 | 90 | 45 |
| ABT-UV60 | 8 | 2 | 0.3 | 90 | 60 |

Dongguan Zhuosheng Machinery Equipment Co., Ltd). The samples were heated at 180 °C for 10 min, then pressed for 2 min at a pressure of five bars. Samples of neat PLA and PBAT, PLA/PBAT blend, PLA/PBAT/TAIC without UV treatment, and PLA/PBAT/TAIC exposed to UV radiation for 15, 30, 45, and 60 min were labeled as PLA, PBAT, AB, ABT-UV0, ABT-UV15, ABT-UV30, ABT-UV45, and ABT-UV60, respectively. Figure 1 is the schematic diagram of the sample preparation process.

## Characterization

### Morphology

The fractured morphology of the samples after being subjected to impact strength (IS) testing was observed through a field emission scanning electron microscope (FESEM Tescan MAIA3) at a SEM HV of 5 kV. A thin layer of gold film was sputtered onto the samples before being examined under the FESEM.

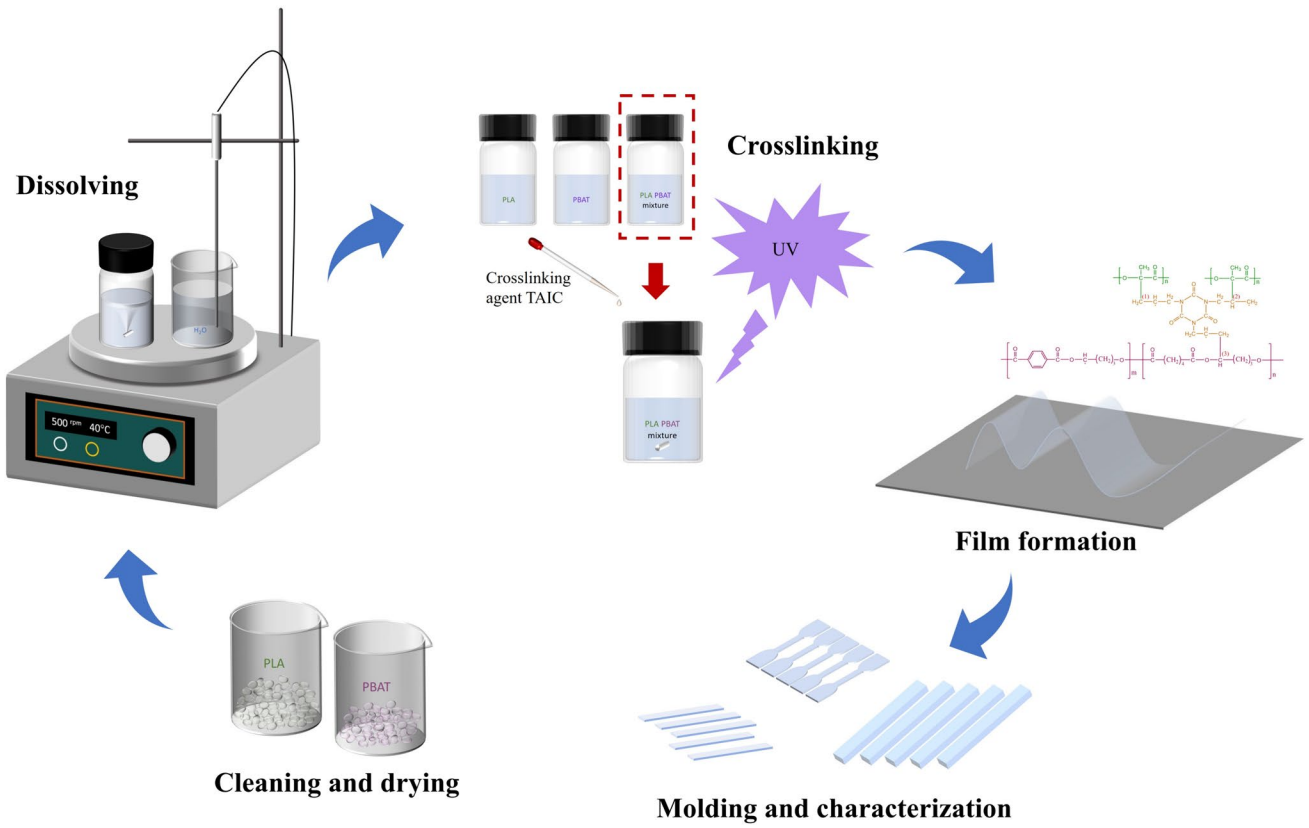


**Fig. 1** Schematic diagram of sample preparation

### Fourier transform infrared spectroscopy

A Fourier transform infrared (FTIR) spectrometer (Spectrum 100, PerkinElmer) was used to determine the interactions among PLA, PBAT, and TAIC. The FTIR curves were recorded in transmittance mode, with a constant spectral resolution of 4 $cm^{-1}$, scanning number of 32, and scanning wavelength that ranged from 600 nm to 4000 nm.

### Mechanical properties

Tensile testing was conducted according to ISO 527 standard, by using INSTRON 5566, a universal testing machine. The samples were molded into a dumbbell shape, with an initial gauge length of 25 mm, width of 4 mm and thickness of 1 mm. They were then conditioned at a temperature of 25 °C and humidity of 50% for 24 h before being tested. The tensile strength and elongation at break results were recorded based on the average results of five samples.

Impact testing was conducted according to ISO 179 by using a Zwick Charpy impact machine with a 1 J hammer. The samples were prepared unnotched with dimensions of 80 x10 x 4 mm. The IS results were recorded as the average value of five samples.

### Thermal transitions

The thermal transitions of the samples were investigated by using a differential scanning calorimeter (PerkinElmer DSC 8000), supplied by Al instruments (Hong Kong) Limited. Samples that weighed approximately 3 mg were placed in aluminum pans for measurement. They were heated from 0 °C to 300 °C at 20 °C/min, at a nitrogen flow rate of 50 ml/min. The Tg was determined by estimating the midpoint in proximity to the change in specific heat (ΔCp). The midpoint of the segment between the onset and offset of Tg was defined as the Tg [17]. The melting point (Tm) is the peak value according to the International Confederation for Thermal Analysis and Calorimetry (ICTAC) standards.

A dynamic mechanical analyzer (DMA Q800, TA, USA) was used to determine the Tg of the samples. The measurement was performed by heating the samples (with dimensions of 60 x 10 x 1 mm) from room temperature to 120 °C at a rate of 5 °C/ min in a 3-point-bend mode.

### Thermogravimetric analysis (TGA)

The thermal stability of samples was evaluated by using a thermalgravimetric analyzer (PerkinElmer TGA 4000 System 100-240 V/50-60HZ), supplied by Labware Analytical Company Limited. The samples were heated from 50 °C to 800 °C at 20 °C/min, at a nitrogen flow rate of 20 ml/min.

## Results and discussion

### Morphology

The scanning electron microscopy images of the fractured surfaces of PLA, PBAT, PLA/PBAT, ABT-UV0, ABT-UV15, ABT-UV30, ABT-UV45, and ABT-UV60 were observed with an FESEM at a magnification of 3 kx. As depicted in Fig. 2(a), the neat PLA has a very smooth fractured surface without any visible plastic deformation, indicating its brittle property. Comparatively, the fractured surface of neat PBAT in Fig. 2(b) shows obvious plastic deformation, which suggests the tough performance of PBAT. Figure 2(c) shows that the AB sample is composed of two phases, the PBAT dispersed phase and the PLA matrix phase. Meanwhile, there is an obvious interfacial separation on the fractured surface, thus indicating low interfacial adhesion between PLA and PBAT. The incompatibility of PLA and PBAT has been reported in previous studies numerous times [18, 19]. The PBAT phase is usually distributed within the PLA matrix in the form of spheres or columns instead of uniformly blending into the PLA. PLA and PBAT are immiscible at the molecular level according to the Gibbs free energy formula:

$$\Delta G_{mix} = \Delta H_{mix} - T\Delta S_{mix}$$

where $\Delta G_{mix}$ is the Gibbs free energy, and $\Delta H_{mix}$ and $\Delta S_{mix}$ represent the enthalpy and entropy changes, respectively. T denotes the temperature (Kelvin) [20]. According to this theory, a negative free energy of mixing homogeneous miscibility in polymer blends is required. The high molecular weight results in negligible mixing entropy. As the mixing enthalpy is positive and there is no specific interaction between these two polymers, the result is the immiscibility of the PLA and PBAT polymers [21]. As depicted in Fig. 2(c), the PLA matrix undergone brittle fracture when an impact force was applied, while the PBAT phase was still continuous and under tension. The PBAT phase was detaching from the PLA matrix at the interface when tension was applied, so gaps and cavities was formed. In the end, the fracture of the PBAT phase occurred, and tough fractures of the PBAT phase formed.

Figure 2(d) shows that there is no obvious difference between ABT-UV0 and AB. However, the fractured surface of ABT-UV15 demonstrates increased compatibility of the PLA and PBAT phases after the sample was exposed to UV light for 15 min, see Fig. 2(e). The width of the gaps that originated from the interfacial detachment is narrower and there are fewer cavities. This result might be due to the crosslinking reaction mechanism as detailed in Section "Mechanism" in which the PLA and PBAT molecular chains started to bond together because of the TAIC and

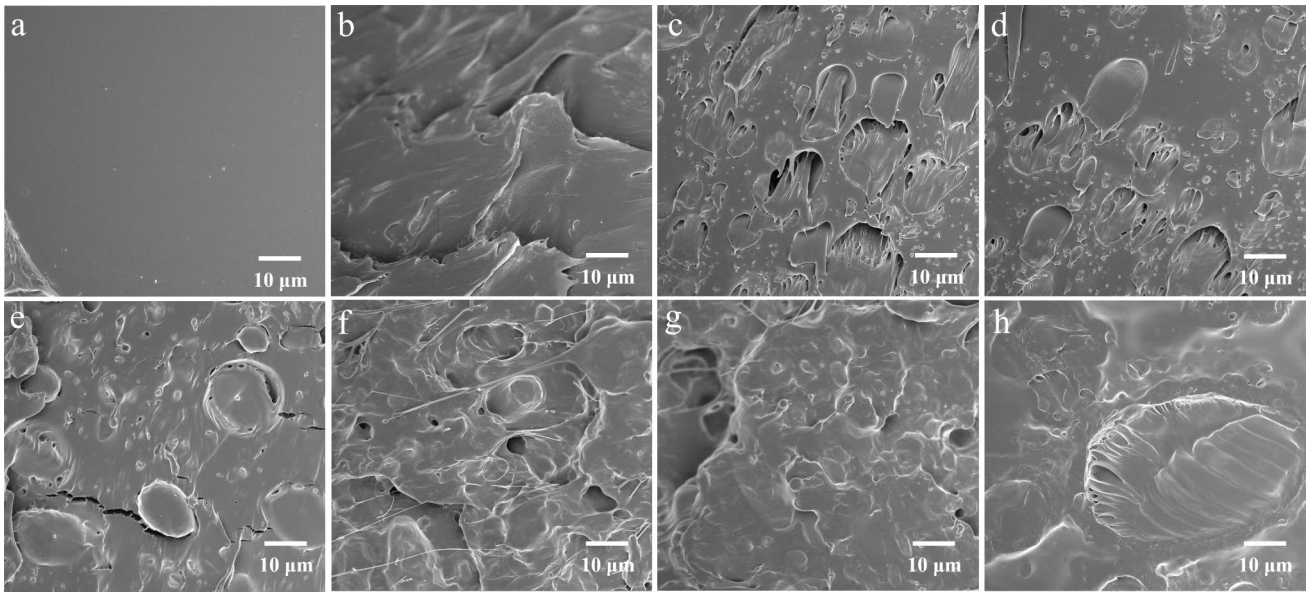


**Fig. 2** Scanning electron microscopy images of **a** neat PLA, **b** neat PBAT, **c** blended PLA/PBAT, **d** untreated PLA/PBAT/TAIC, **e** PLA/PBAT/TAIC exposed to UV light for 15 min, **f** PLA/PBAT/TAIC exposed to UV light for 30 min, **g** PLA/PBAT/TAIC exposed to UV light for 45 min, and **h** PLA/PBAT/TAIC exposed to UV light for 60 min

UV radiation. Figure 2(e) to (h) show that the two-phase interfaces cannot be differentiated from the fractured surface images as the UV radiation exposure time is over 30 min. This result indicates that as the crosslinking reaction progressed, the PBAT molecular chains distributed more uniformly in the PLA matrix. In contrast to the brittle and smooth fractured surface of the neat PLA, the fractured sections of ABT-UV30 and ABT-UV45 exhibit more fibrils pulling out, which suggests the enhanced toughness of the samples. However, there is less plastic deformation on the fractured surface of ABT-UV60. This is likely because excessive crosslinking reactions can increase rigidity, thus reducing the toughness of the sample.

## Fourier transform infrared spectroscopy

The chemical structures of PLA, PBAT, TAIC and ABT-UV30 were characterized by FTIR spectroscopy, as shown in Fig. 3. In the case of PLA, the three peaks at 1044 $cm^{-1}$, 1076 $cm^{-1}$, and 1183 $cm^{-1}$ are related to the stretching vibrations of the ether groups (C–O–C). The characteristic peak at 1751 $cm^{-1}$ is assigned to the stretching vibrations of the carbonyl groups (C = O). The two peaks that appear at 2855 $cm^{-1}$ and 2925 $cm^{-1}$ belong to the stretching vibrations of the tertiary carbon and hydrogen bonds (C-H) on backbones [22]. The two characteristic peaks at 2942 $cm^{-1}$ and 2995 $cm^{-1}$ are the symmetric and asymmetric stretching vibrations of the methyl groups ($CH_3$) in saturated hydrocarbons, which are clearly visible in all of the FTIR spectra [23]. For the neat PBAT, the characteristic peak at 1018 $cm^{-1}$ is due to the vibrations of the hydrogen atom of the aromatic ring. Peaks that appear at 1104 $cm^{-1}$ and 1267 $cm^{-1}$ are the symmetric stretching vibrations of the carbon and oxygen groups (C–O). The characteristic peaks at 1409 $cm^{-1}$ and 2948 $cm^{-1}$ are assigned to the in-plane bending vibrations and the asymmetric stretching vibrations of the methylene groups ($CH_2$), respectively. The bands at 1504 $cm^{-1}$ and 1711 $cm^{-1}$ are the skeletal vibrations of the aromatic ring and the stretching vibrations of the C = O. In the FTIR curve of TAIC, the peaks at 1376 $cm^{-1}$ and 1756 $cm^{-1}$ are the tertiary amide absorption vibrations. The characteristic peaks at 1653 $cm^{-1}$ and 1695 $cm^{-1}$ are attributed to the stretching vibrations of the carbon-carbon double bonds (C = C) and the stretching vibrations of C = O [12]. In the curve of ABT-UV30, the peak of the C = C stretching vibrations of TAIC at 1653 $cm^{-1}$ is no longer there. This indicates the breakage of the C = C bond in TAIC under UV radiation and the formation of TAIC radicals. In addition, there are new bands at 3506 $cm^{-1}$, which can be assigned to a hydroxyl group (–OH). The formation of hydroxyl groups is attributed to thermal degradation of PLA and PBAT macromolecules during the UV radiation or melting process [24].

## Mechanism

The mechanisms of the crosslink reaction and molecular chain breakdown brought on by the UV light are shown in

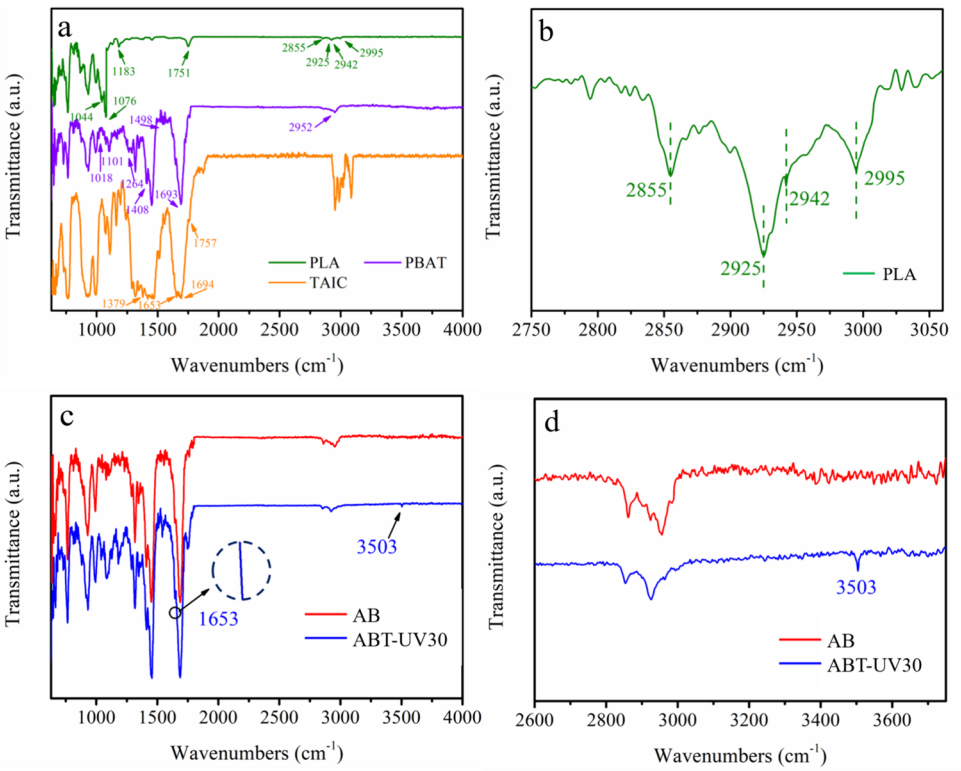


**Fig. 3** FTIR of **a** PLA, PBAT, and TAIC, **b** enlarged view of PLA, **c** AB and ABT-UV30, and **d** enlarged view of AB and ABT-UV30

Fig. 4. Figure 4(a) describes the two steps of the crosslink reaction. In the first step, the carbon and hydrogen (C-H) bonds on the PLA backbones are broken under the influence of UV light. PLA free radicals formed because of the loss of protons of the tertiary carbon. Meanwhile, UV radiation also contributes to the formation of TAIC and PBAT radicals. In the second step, the PLA and PBAT free radicals combined with TAIC radicals mainly in three types of reactions as shown in Fig. 4(a). The numbers 1, 2, and 3 which represent the three types of reactions also indicate the difficulty of the reaction. It is more difficult for Reaction Type 2 to happen than Reaction Type 1 mainly due to the steric hindrance. Malinowski et al. [22] reported that PLA has higher susceptibility to electromagnetic radiation than PBAT when radiation is used to promote chemical reactions. The presence of aromatic groupings in PBAT macromolecular chains can absorb some of the electromagnetic radiation and dissipate it in the form of heat. This so-called protective effect deactivates some of the active sites. As a result, it is more difficult for PBAT to form free radicals, and PBAT is less prone to have a crosslink reaction when compared to PLA. Therefore, it is more difficult for Reaction Type 3 to occur in comparison with Reaction Type 2. In addition to crosslink reactions, the chain scission of PLA may also occur when the samples are excessively exposed to UV radiation, as PLA is sensitive to UV radiation. This could be inferred from the new formation of hydroxyl group bands on the FTIR curves of ABT-UV30 as discussed in Section "Fourier transform infrared spectroscopy". Besides, samples exposed to UV light for a prolonged period also lose some of their mechanical and thermal properties, as will be discussed in more details in Sections "Mechanical properties" and "Thermal stability".

## Mechanical properties

The tensile strength, modulus, elongation at break and impact strength of PLA, PBAT, AB, ABT-UV0, ABT-UV15, ABT-UV30, ABT-UV45, and ABT-UV60 were tested and the results are listed in Table 2. The results are also plotted in Fig. 5 to visually show the changes in these mechanical properties. As shown in Table 2, the tensile strength of neat PLA is 65.7 MPa and the elongation at break is only 4.4%, indicating that PLA is a strong but brittle polymer at room temperature. Comparatively, PBAT has a low tensile strength of 16.4 MPa and a high elongation at break of 611.5%, which suggest its weak and flexible properties. As shown in Fig. 5, the elongation at break of AB is increased to 10.4%, which is approximately 2.4 times higher than neat PLA. This shows that the addition of PBAT can increase the flexibility of PLA. Meanwhile, the tensile strength and modulus of AB are slightly decreased compared to neat PLA, which could be brought on by the defects resulting from the two-phase interface separation. The effect of PBAT on the mechanical

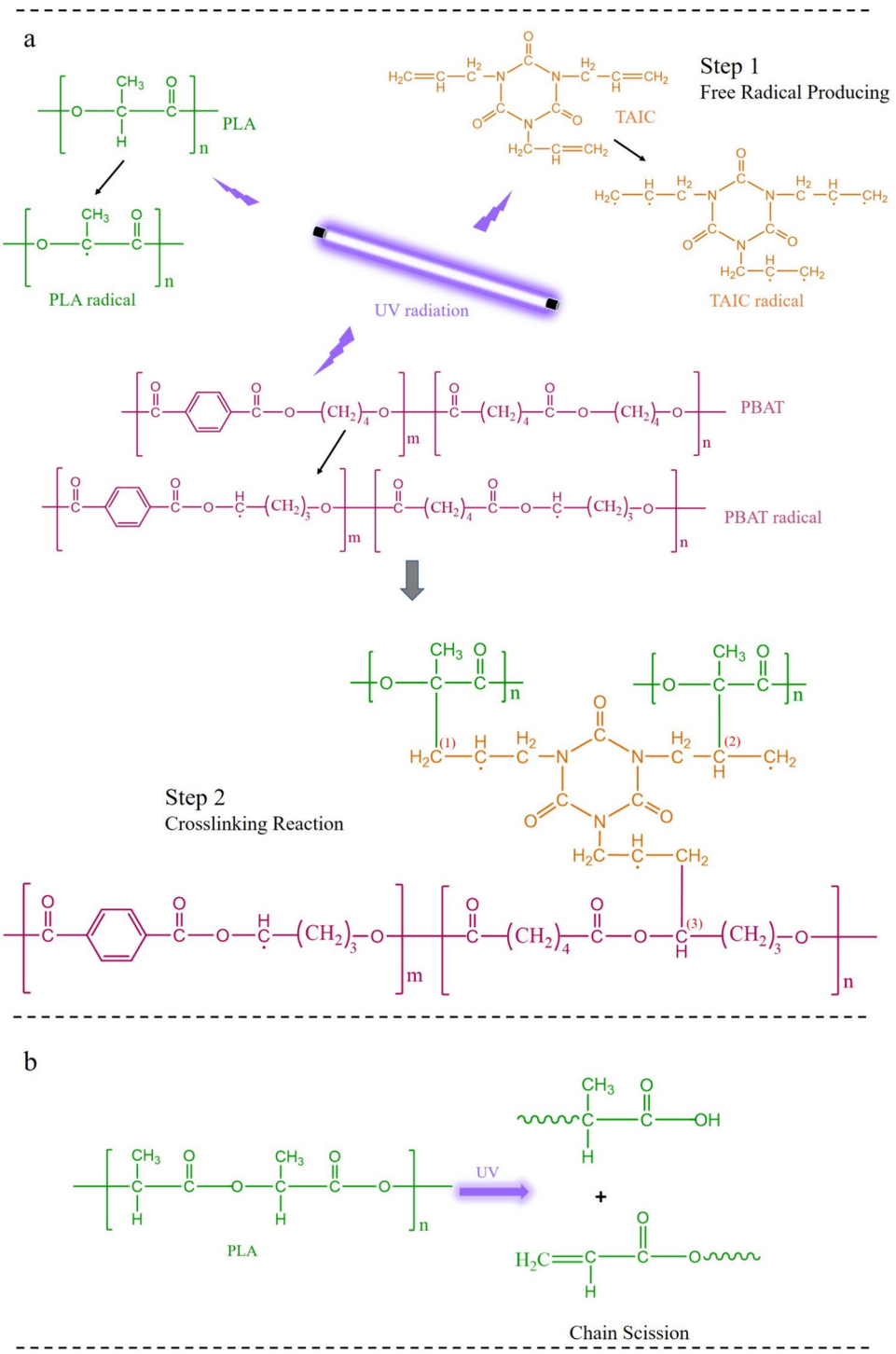


**Fig. 4** **a** Crosslinking reaction processes, and **b** degradation of PLA macromolecular chain

properties of PLA is consistent with the results reported in previous studies [25, 26].

After the addition of TAIC, both the tensile strength and the modulus of samples are decreased compared to those of AB. The PLA and PBAT molecular chains were lubricated by the miniscule TAIC molecules, which declined the entanglement and connectivity between the chains and consequently reduced the tensile strength and modulus of ABT-UV0. The tensile strength and elongation at break of the samples are increased initially as the UV radiation period was increased from 0 to 30 min, but started to decline when the UV radiation time exceeded 30 min. The crosslinked spatial network developed during the crosslink reaction may have contributed to the increase in tensile strength of ABT-UV15, ABT-UV30,

**Table 2** Mechanical properties of PLA, PBAT, AB, ABT-UV0, ABT-UV15, ABT-UV30, ABT-UV45, and ABT-UV60

| Sample name | Tensile strength at maximum load (MPa) | Elongation at break (%) | Modulus (MPa) | Unnotched impact strength (KJ/m$^2$) |
|---|---|---|---|---|
| PLA | 65.7 ± 2.9 | 4.4 ± 0.8 | 1452.4 ± 27.4 | 2.9 ± 0.1 |
| PBAT | 16.4 ± 1.4 | 611.5 ± 15.7 | 56.1 ± 2.2 | 65.2 ± 4.5 |
| AB | 57.7 ± 3.2 | 6.8 ± 0.4 | 1431.3 ± 15.6 | 7.5 ± 1.5 |
| ABT-UV0 | 52.6 ± 3.7 | 10.4 ± 1.8 | 992.3 ± 18.1 | 7.4 ± 0.7 |
| ABT-UV15 | 43.7 ± 1.6 | 16.5 ± 1.2 | 640.5 ± 13.9 | 21.2 ± 1.9 |
| ABT-UV30 | 48.4 ± 3.2 | 17.1 ± 0.6 | 634.0 ± 25.1 | 24.4 ± 1.7 |
| ABT-UV45 | 40.1 ± 3.2 | 16.1 ± 1.4 | 648.6 ± 21.0 | 20.6 ± 1.5 |
| ABT-UV60 | 38.8 ± 2.1 | 14.2 ± 0.2 | 990.0 ± 31.8 | 12.2 ± 1.6 |

ABT-UV45, and ABT-UV60. UV radiation can, however, also cause chain scissions in the PLA macromolecular chains, which reduces the tensile strength of the samples. Overall, the sample of ABT-UV30 demonstrated the superior strength and flexibility of 48.4 MPa and 17.1%.

As depicted in Table 2; Fig. 5(d), the toughness of PBAT is significantly higher than that of PLA, with unnotched impact strength values of 65.2 KJ/m$^2$ and 2.9 KJ/m$^2$, respectively. The impact strength of AB was increased by 158.6% by the addition of PBAT at a mass proportion of 20%. As the UV radiation time was increased from 0 to 30 min, the impact strength was initially increased then decreased once the UV radiation time exceeded 30 min. The toughening effect of PBAT and the increased compatibility of PLA and

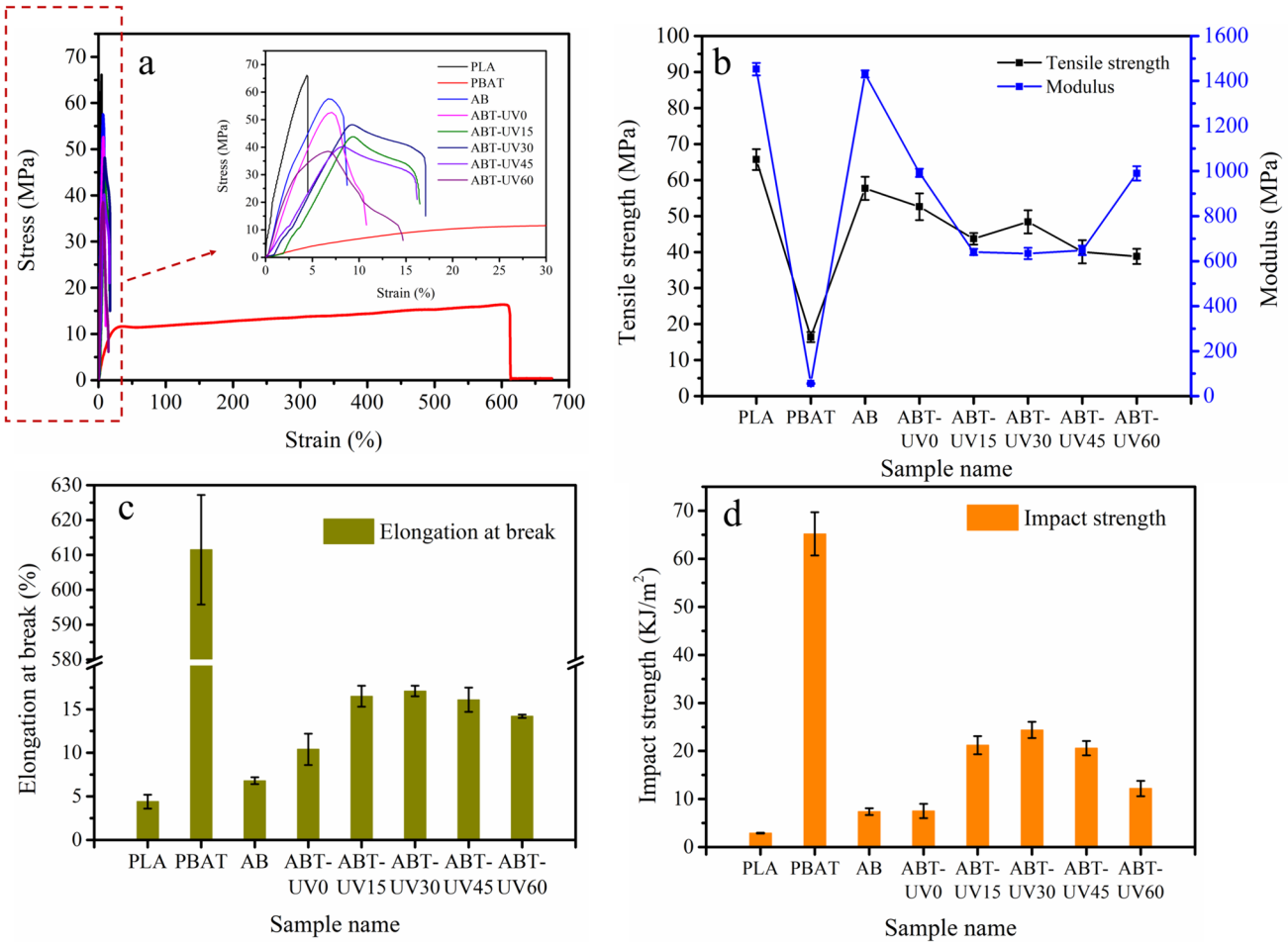


**Fig. 5** Mechanical properties of PLA, PBAT, AB, ABT-UV0, ABT-UV15, ABT-UV30, ABT-UV45, and ABT-UV60. **a** Stress-strain curves, **b** tensile strength and modulus, **c** elongation at break, and **d** impact strength

**Table 3** Thermal transition temperatures

| Sample name | Tg-PLA (°C) | Tm-PLA (°C) | Tm-PBAT (°C) |
|---|---|---|---|
| PLA | 63.4 | 164.7 | N/A |
| PBAT | N/A | N/A | 127.6 |
| AB | 55.3 | 161.2 | 127.4 |
| ABT-UV0 | 52.2 | 154.8 | 139.5 |
| ABT-UV15 | 66.6 | 154.3 | 137.4 |
| ABT-UV30 | 67.9 | 153.4 | 140.4 |
| ABT-UV45 | 68.7 | 152.1 | 152.1 |
| ABT-UV60 | 72.9 | 152.4 | 152.4 |

PBAT were the key contributors to the improvement in the impact strength. However, the formation of the crosslinking network can also lead to rigidity, which reduces the impact strength of the samples, which corresponding to the results shown in stress-strain curves.

## Thermal transitions

Thermal transition properties can greatly influence the mechanical performance of composites. Specifically, the Tg represents the transition point between the glassy and brittle state and the elastic and ductile state. To understand the thermal transitions of the samples, the DSC and DMA tan delta-temperature thermograms of PLA, PBAT, AB, ABT-UV0, ABT-UV15, ABT-UV30, ABT-UV45, and ABT-UV60 were investigated. The Tg obtained from the tan delta-temperature curves and Tm obtained from the DSC thermograms are detailed in Table 3 and illustrated in Fig. 6. According to Table 3, PLA has a Tg of 63.4 °C, which shows that PLA has brittle behavior at ambient temperatures below 63.4 °C. The non-elastic nature of the material is also demonstrated by the large tan delta value shown in Fig. 6(c) [27]. According to [28], the Tg of PBAT is at around − 35 °C, which means PBAT maintains its elastic and ductile performances at room temperature. As shown in Table 3, the addition of PBAT reduced the Tg of PLA in AB from 63.4 °C to 55.3 °C. The lower Tg shows that the addition of flexible PBAT molecular chains improved the mobility of PLA molecular chains in the amorphous area. As a result, PLA molecular chains require a lower temperature to complete the phase transition, i.e., changing from a rigid glassy state to a highly elastic state. The Tg of the samples was gradually increased as the UV radiation exposure period was increased from 0 to 60 min. This is because the crosslinking reaction produced a crosslinked spatial network, which made it difficult for polymer chains to move locally and thus the Tg was increased [29]. The Tg curve of the ABT samples was not clearly apparent on the DSC thermograms, possibly as a result of the varying degrees of restrictions of the different crosslinking networks on the mobility of the PLA molecular chains in the amorphous region. As a result, the PLA molecular chains began to move over a wider temperature

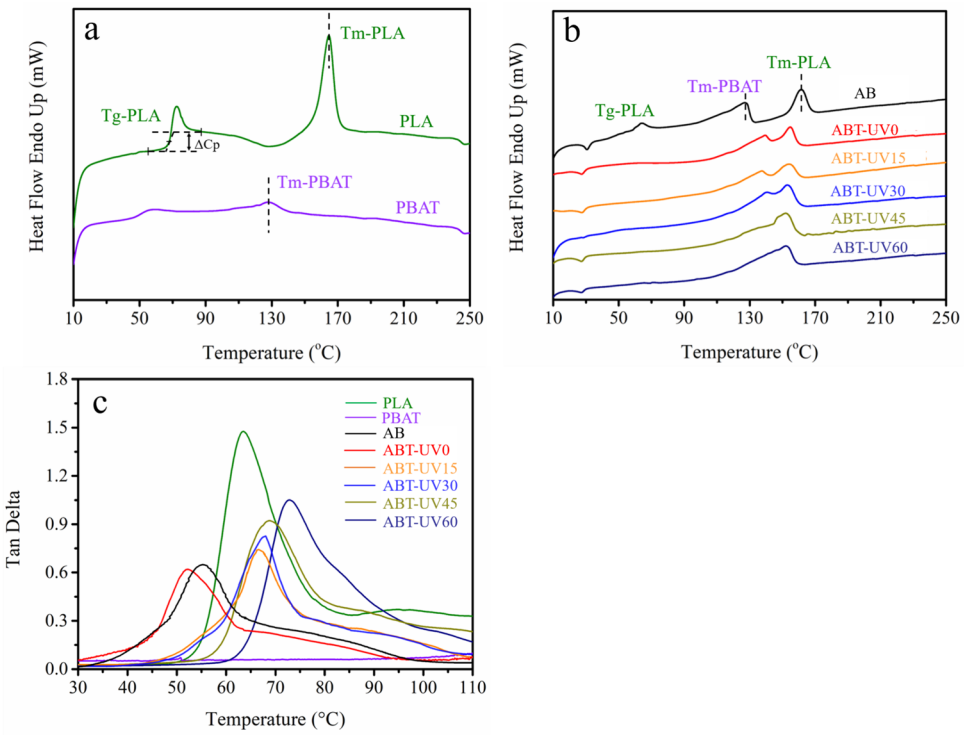


**Fig. 6** DSC thermograms of **a** PLA and PBAT, and **b** AB, ABT-UV0, ABT-UV15, ABT-UV30, ABT-UV45 and ABT-UV60. **c** DMA thermograms of all samples

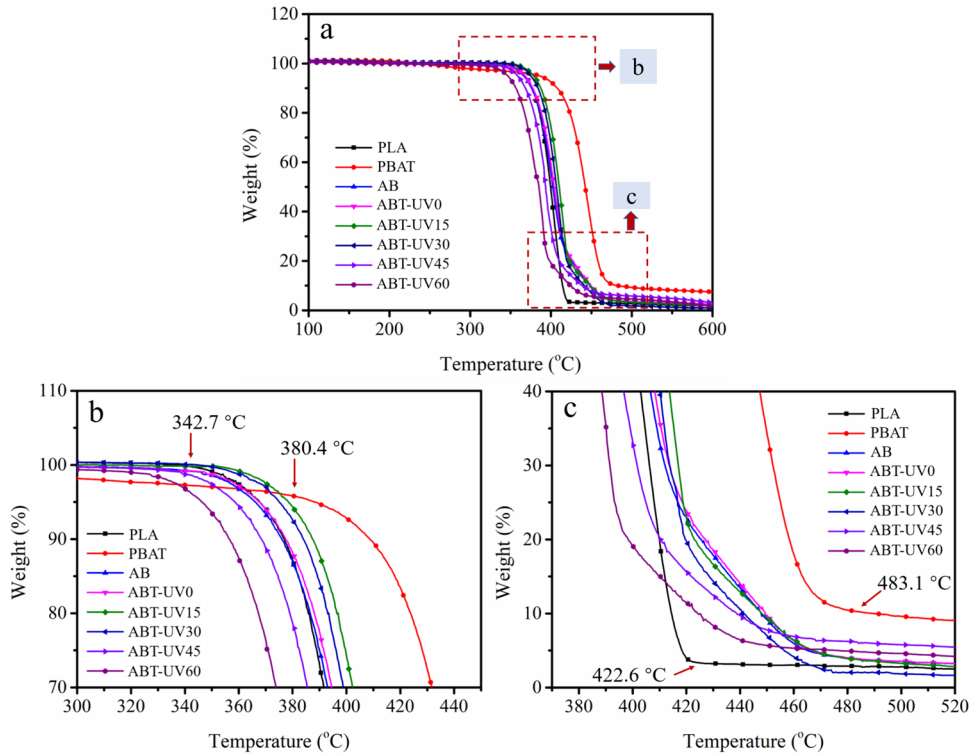


**Fig. 7** TGA thermograms of PLA, PBAT, AB, ABT-UV0, ABT-UV15, ABT-UV30, ABT-UV45, and ABT-UV60: **a** full image, **b** enlarged view of onset degradation process, and **c** enlarged view of offset degradation process

range, which was reflected in the inconspicuous exothermic trend on the DSC thermograms.

Table 3 shows that the melting point temperature (Tm) of neat PLA is 164.7 °C, while that of PBAT is only 127.7 °C. Bunn [31] reported that PBAT with many methylene groups has a very low Tm as the methylene groups are very light and flexible so very less thermal energy is required to make the chain move. The Tm of PLA is slightly reduced in the AB sample. This is because the addition of flexible PBAT molecular chains enhanced the mobility of the PLA molecular chains, which interfered with their crystallization process, thus resulting in a decrease in Tm [30]. As the length of the UV radiation was increased from 0 to 60 min, the crosslinking reaction increasingly progressed. The Tm of PLA was decreased while that of PBAT was increased at the same time. On the one hand, the crosslinked spatial network in PLA reduced the chain orientation, and a low molecular packing efficiency of the crystals can reduce the melting point. On the other hand, when the crystals start to melt, the rigid molecular chain needs to move as a whole, while in a flexible chain, distortion at one point can produce waves along the chain arising from the movement of the entire chain [31]. The introduction of flexible PBAT chains enhances the movement of the entire chain, thus reducing the Tm of PLA. The Tm of PBAT was increased at the same time, because a higher thermal energy is required to break the bonds of the crosslinked network and cause movement of the individual PBAT chains. The crosslinking density influences the melting point of each type of polymer. As a result, the melting point peaks of PLA and PBAT became increasingly closer and eventually coincide with a longer UV radiation time. The crosslinking reaction resulted in sufficiently strong interactions between the PLA and PBAT polymers.

## Thermal stability

The thermal degradation performance of PLA, PBAT, AB, ABT-UV0, ABT-UV15, ABT-UV30, ABT-UV45, and ABT-UV60 was determined by using a TGA. Figure 7(a) shows that both the PLA and PBAT polymers underwent a one-step thermal degradation process. The former started to degrade at 342.7 °C and the degradation curve tended to flatten at 422.6 °C, while PBAT began to degrade at 380.4 °C and had almost no residue at 483.1 °C. PBAT maintains a higher thermal degradation temperature than PLA due to the presence of an aromatic structure in its macromolecular chains, and PBAT has a longer segment compared to PLA. Figure 7 clearly shows that samples of AB, ABT-UV0, ABT-UV15, ABT-UV30, ABT-UV45, and ABT-UV60 underwent a two-step thermal degradation process, which corresponds to the thermal degradation process of PLA and PBAT [16]. Figure 7(b) is the enlarged view of the onset of the degradation process, which shows that AB and ABT-UV0 have a very similar onset degradation temperature as PLA due to the dominant role of PLA in the sample. As the duration of the UV radiation was increased from 0

to 60 min, the onset degradation temperature was initially increased, then decreased when the UV exposure time was over 15 min. The onset degradation temperature of ABT-UV 15 was increased to around 350 °C, which indicates that the crosslinking structure can increase the degradation temperature. However, as the UV radiation time was prolonged to 60 min, the onset degradation temperature was reduced to 326.9 °C, which is even lower than that of neat PLA. This might because the prolonged UV exposure can also cause the degradation of PLA, which promote its thermal decomposition. The offset degradation is shown in Fig. 7(c), where the samples with a lower onset degradation temperature also have a lower offset degradation temperature.

## Conclusion

The fabrication of fully biodegradable PLA/PBAT blend with a crosslinked network structure was carried out in this study. The results show that the introduction of PBAT can improve the toughness and flexibility of PLA. The compatibility of PLA and PBAT was enhanced due to the formation of a crosslinked network structure. ABT-UV30 overall has the optimal mechanical properties. The elongation at break and impact strength of this sample were increased 3.9 times and 8.4 times, respectively, when compared to PLA. The Tg of the samples was increased gradually when the UV radiation exposure time was extended from 0 to 60 min. At the same time, the melting point temperature of PBAT was also increased gradually until it is eventually the same as that of PLA. The TGA thermograms show that an appropriate amount of UV radiation exposure can increase the thermal degradation temperature, while excessive UV radiation exposure can reduce the thermal degradation temperature of the samples. The PLA-based biodegradable materials with high toughness can be used as an alternative for non-biodegradable plastics, which can be applied in packaging, disposable box & bottles, tableware, textiles, and flexible intelligent electronics. Although the UV radiation is necessary to induce the crosslink reaction, excessive UV radiation can also degrade the PLA molecular chain, which might decrease the thermal stability of the blend. Besides, the introduction of flexible PBAT chain of the structure can increase the flexibility of the PLA/PBAT blend. However, the crosslink structure can also lead to rigidity, reducing the toughening and plasticizing effects of PBAT.

**Acknowledgements** This study was supported by Innovation and Technology Fund (Ref No. PRP/104/20TI) of Hong Kong Special Administrative Region, Wuyi University-Hong Kong Joint Research Fund under the Hong Kong Polytechnic University and Wuyi University collaborative flamework agreement, Wuyi University–Hong Kong/Macau Joint Research Funds (2019WGALH05). The authors also appreciated the PhD scholarship provided by the Hong Kong Polytechnic University.

**Author contributions** Bian Xueyan: Conceptualization, Methodology, Investigation, Writing - original draft. Fan Suju: Investigation, Writing - review & editing. Xia Gang: Investigation, Writing - review & editing. Xin John Haozhong: Conceptualization, Methodology, Writing - review & editing, Resources. Jiang Shouxiang: Writing - review & editing, Project administration, Resources.

**Funding** Open access funding provided by The Hong Kong Polytechnic University

## Declarations

**Competing interest** The authors declare that they have no known competing financial interests or personal relationships that could have appeared to influence the work reported in this paper.

**Open Access** This article is licensed under a Creative Commons Attribution 4.0 International License, which permits use, sharing, adaptation, distribution and reproduction in any medium or format, as long as you give appropriate credit to the original author(s) and the source, provide a link to the Creative Commons licence, and indicate if changes were made. The images or other third party material in this article are included in the article's Creative Commons licence, unless indicated otherwise in a credit line to the material. If material is not included in the article's Creative Commons licence and your intended use is not permitted by statutory regulation or exceeds the permitted use, you will need to obtain permission directly from the copyright holder. To view a copy of this licence, visit http://creativecommons.org/licenses/by/4.0/.

## References

1. Geyer R, Jambeck JR, Law KL (2017) Production, use, and fate of all plastics ever made. Sci Adv 3(7):e1700782
2. Irmak S (2017) Biomass as raw material for production of high-value products. In: Tumuluru JS (ed) Biomass volume estimation and valorization for energy. IntechOpen, Rijeka (Ch. 9)
3. Zhou Y et al (2021) A facile and sustainable approach for simultaneously flame retarded, UV protective and reinforced poly(lactic acid) composites using fully bio-based complexing couples. Compos Part B: Eng 215:108833
4. Wang W et al (2021) 3D printing of PLA/n-HA composite scaffolds with customized mechanical properties and biological functions for bone tissue engineering. Compos B Eng 224:109192
5. Meng L et al (2019) Preparation, microstructure and performance of poly (lactic acid)-poly (butylene succinate-co-butyleneadipate)-starch hybrid composites. Compos B Eng 177:107384
6. Nofar MR et al (2020) Ductility improvements of PLA-based binary and ternary blends with controlled morphology using PBAT, PBSA, and nanoclay. Compos B Eng 182:107661
7. Jalali A et al (2020) Peculiar crystallization and viscoelastic properties of polylactide/polytetrafluoroethylene composites induced by in-situ formed 3D nanofiber network. Compos B Eng 200:108361
8. Jia YW et al (2020) Synergy effect between quaternary phosphonium ionic liquid and ammonium polyphosphate toward flame retardant PLA with improved toughness. Compos B Eng 197:108192
9. Lay M et al (2019) Comparison of physical and mechanical properties of PLA, ABS and nylon 6 fabricated using fused deposition modeling and injection molding. Compos B Eng 176:107341
10. Ikada Y et al (1987) Stereocomplex formation between enantiomeric poly(lactides). Macromolecules 20(4):904–906

11. Tang Z et al (2012) The crystallization behavior and mechanical properties of polylactic acid in the presence of a crystal nucleating agent. J Appl Polym Sci 125(2):1108–1115
12. Shaffer S et al (2014) On reducing anisotropy in 3D printed polymers via ionizing radiation. Polymer 55(23):5969–5979
13. Tsou C-H et al (2018) Preparation and characterization of poly(lactic acid) with adipate ester added as a plasticizer. Polym Polym Compos 26(8–9):446–453
14. Kobayashi et al (2004) Polylactic acid resin composition and method for producing the same. Japan Patent JP2004250549A
15. Balla E et al (2021) Poly(lactic acid): a versatile Biobased Polymer for the future with multifunctional properties—from Monomer Synthesis, polymerization techniques and Molecular Weight increase to PLA applications. Polymers 13(11):1822
16. Fu Y et al (2020) Biodegradation Behavior of Poly(Butylene Adipate-Co-Terephthalate) (PBAT), poly(lactic acid) (PLA), and their blend in freshwater with sediment. Molecules 25(17):3946
17. Parodi E et al (2017) Glass transition temperature versus structure of polyamide 6: A flash-DSC study. Thermochim Acta 657:110–122
18. Malinowski RK (2020) Studies on the uncrosslinked fraction of PLA/PBAT blends modified by electron radiation. Materials (Basel) 13(5):1068
19. Wu D et al (2021) Effect of the multi-functional epoxides on the thermal, mechanical and rheological properties of poly(butylene adipate-co-terephthalate)/polylactide blends. Polym Bull 78:1–25
20. Koning C et al (1998) Strategies for compatibilization of polymer blends. Prog Polym Sci 23(4):707–757
21. Yue Ding BL, Ji J (2020) Compatibilization strategies of PLA-Based biodegradable materials. Progress Chem 32(6):738–751
22. Malinowski R, Moraczewski K, Raszkowska-Kaczor A (2020) Studies on the Uncrosslinked Fraction of PLA/PBAT blends modified by Electron Radiation. Materials 13(5):1068
23. Mehmet Kodal AAW, Ozkoc G (2018) The mechanical, thermal and morphological properties of γ-irradiated PLA/TAIC and PLA/OvPOSS. Radiat Phys Chem 153:214–225
24. Rytlewski P et al (2010) Influence of some crosslinking agents on thermal and mechanical properties of electron beam irradiated polylactide. Radiat Phys Chem 79(10):1052–1057
25. Ming M et al (2022) Effect of polycarbodiimide on the structure and mechanical properties of PLA/PBAT blends. J Polym Res 29:371
26. Mohammadi M et al (2021) Morphological and Rheological Properties of PLA, PBAT, and PLA/PBAT Blend nanocomposites containing CNCs. Nanomaterials 11(4):857
27. Wasti S et al (2021) Influence of plasticizers on thermal and mechanical properties of biocomposite filaments made from lignin and polylactic acid for 3D printing. Compos Part B: Eng 205:108483
28. Pietrosanto A et al (2020) Evaluation of the suitability of Poly(Lactide)/Poly(butylene-Adipate-co-Terephthalate) blown films for Chilled and Frozen Food Packaging Applications. Polymers 12(4):804
29. Ding Y et al (2021) Effect of talc and diatomite on compatible, morphological, and mechanical behavior of PLA/PBAT blends. e-Polymers 21:234–243
30. Kumar M et al (2010) Effect of glycidyl methacrylate (GMA) on the thermal, mechanical and morphological property of biodegradable PLA/PBAT blend and its nanocomposites. Bioresour Technol 101(21):8406–8415
31. Bunn CW (1996) The melting points of chain polymers. J Polym Sci Part B: Polym Phys 34(5):799–819


**Publisher's Note** Springer Nature remains neutral with regard to jurisdictional claims in published maps and institutional affiliations.